Environment International 136 (2020) 105462

Contents lists available at ScienceDirect

Environment International

journal homepage: www.elsevier.com/locate/envint

Occurrence of multiple classes of emerging photoinitiators in indoor dust from E-waste recycling facilities and adjacent communities in South China and implications for human exposure

Juan Li[a], Wenzheng Li[a], Xiaoming Gao[b], Liangying Liu[a], Mingjie Shen[a], Hui Chen[a], Mingshan Zhu[a], Lixi Zeng[a,*], Eddy Y. Zeng[a]

[a] Guangdong Key Laboratory of Environmental Pollution and Health, School of Environment, Jinan University, Guangzhou 511443, China
[b] Quality Management Center, National Institutes for Food and Drug Control, Beijing 102629, China

ARTICLE INFO

Handling Editor: Adrian Covaci

Keywords:
Photoinitiators
E-waste recycling facility
Indoor dust
Human exposure
Estimated daily intake

ABSTRACT

Photoinitiators (PIs) are indispensable additives in photopolymerization. PI-containing consumables, such as adhesives, coatings, UV-cured inks and light-sensitive materials, are widely used in various electronic products. Nevertheless, there is no information concerning the identification of PIs as emerging contaminants from e-waste recycling. In this study, 25 PIs, including 9 benzophenones (BZPs), 8 amine coinitiators (ACIs), 4 thioxanthones (TXs) and 4 phosphine oxides (POs), were analyzed in indoor dust from typical e-waste recycling facilities and adjacent rural communities, as well as from control urban communities. All 25 target PIs were detected in e-waste dust, while only 17 and 15 of the 25 target PIs were detected in local home dust and urban home dust, respectively. The PIs detected in all dust samples were dominated by BZPs and POs, followed by ACIs and TXs. Most PIs exhibited significantly higher levels in e-waste dust than local or urban home dust. The influence of PI contamination on the local household environment by dust diffusion and transport from near e-waste recycling facilities may be lower due to the low volatility of most PIs. Characteristic composition profiles of PIs for indoor dust from the e-waste recycling area were identified and compared to those from the control area. Significant correlations were found among almost all the frequently detected PIs in the e-waste dust, indicating their similar application in electronic products and common emission from e-waste recycling. The estimated daily intakes of PIs via dust ingestion for the e-waste dismantling workers, as determined by using Monte Carlo analysis, were several times higher than those for the local adult residents and the general urban adult residents, which should be an emerging concern. To the best of our knowledge, this is the first report showing that e-waste dismantling/recycling activities lead to largely common releases of a wide range of multiple classes of PIs.

1. Introduction

Photoinitiators (PIs) are mainly used as additives in photopolymerization to generate active substances during the optical absorption process (Matsubara and Ohtani, 2007). Photopolymerization is mainly applied in light-sensitive, UV-curable materials, such as ink, coatings, and adhesives (Ibrahim et al., 2013). Generally, the commonly used PIs can be categorized as benzophenones (BZPs), amine coinitiators (ACIs), thioxanthones (TXs) and phosphine oxides (POs) (Gallart-Ayala et al., 2011; Jung et al., 2013; Williams et al., 2000). China is one of the world's largest PI manufacturers, and total annual production volume was as high as 29 thousand tonnes in 2007 (Jin, 2011). It was estimated that annual discharges of PIs to the environment via the usage and disposal of UV curable resins and food contact materials in China were 307 and 9.57 tonnes, respectively (Liu et al., 2015). Although there are no current statistics on the overall production volume of PIs worldwide, increased production is expected due to the enormous demand of photopolymerization-related products.

Since 2-isopropyl thioxanthone (2-ITX), one of the PI congeners, was first identified at high concentrations (120–300 μg/L) in Nestle and other liquid milks in Europe (Network, 2005), people began to pay attention to their environmental endpoints. Subsequent studies reported that several PIs including 2-ITX, benzophenone (BP), and 2-ethylhexyl-4- (dimethylamino)benzoate (EHDAB) were also found in food packaging materials and foodstuffs (Bradley et al., 2013; Gallart-Ayala et al., 2013; Liu and Mabury, 2019a). Available toxicological

* Corresponding author.
E-mail address: lxzeng@jnu.edu.cn (L. Zeng).

https://doi.org/10.1016/j.envint.2020.105462
Received 4 November 2019; Received in revised form 23 December 2019; Accepted 2 January 2020
Available online 07 January 2020

studies, although limited in numbers, have demonstrated the endocrine disrupting effects and even potential carcinogenicity of multiple PIs (Kitchin and Brown, 1994; Morohoshi et al., 2005; Peijnenburg et al., 2010; Reitsma et al., 2012). For example, TXs (2-ITX and 2,4-diethylthioxanthone, DETX) had antiestrogenic and antiandrogenic activities (Peijnenburg et al., 2010; Reitsma et al., 2012), while BZPs, such as methyl-2-(benzoyl)benzoate (MBB), 1-hydroxycyclohexyl phenyl ketone (PI-184) and 2,2-dimethoxy-2-phenylacetophenone (PI-651), and ACIs, such as EHDAB and 2-methyl-4′-(methylthio)-2-morpholinopropiophenone (PI-907), had estrogenic activities (Morizane et al., 2015; Morohoshi et al., 2005). More importantly, evidences have showed that BZPs were associated with some adverse aspects of human semen quality (Louis et al., 2015). Besides, both BP and 4,4′-bis(dimethylamino) benzophenone (Michler's ketone, MK) were found to facilitate potential carcinogenicity and DNA damage at exposure levels of ~ 300 ng/g and 150 μg/g, respectively, in animal studies (Kitchin and Brown, 1994; Rhodes et al., 2007). As such, in spite of allowable PIs residue amounts in packaged food, in EU-legislated documents (Gil-Vergara et al., 2007), MK was listed as an inadvisable additive used in printing inks applied to paper or paperboard food packaging materials (Council, 2006; Japan, 2006). In addition, novel POs can exert great cytotoxic and genotoxic effects. It was found that 2,4,6-trimethylbenzoyldiphenyl-phosphine oxide (TPO) was ten times more cytotoxic than ethyl-4-dimethylaminobenzoate (EDMAB), which is a well-known PI congener in the ACI group (Landuyt et al., 2015; Manojlovic et al., 2017).

Despite the potential toxicity of some PIs gradually becoming clear, information on their environmental occurrences and human exposure still remains largely unknown. To our knowledge, there are only two reports concerning the environmental contamination of PIs. Elevated concentrations of PIs in food packaging materials, indoor dust and sewage sludge were reported in China previously (Liu et al., 2015) and in Canada recently (Liu and Mabury, 2019a). In addition, human exposure to PIs was also reported by previous studies (Liu and Mabury, 2018, 2019b; Zhang et al., 2013) and our work group (Li et al., 2019). The ubiquitous existence of PIs (423–2870 pg/mL) in human sera from U.S. donors indicated significant human exposure to these emerging contaminants (Liu and Mabury, 2018). Recently, we surprisingly found prevailing prenatal exposure to PIs in pregnant women in South China, thus raising an important concern for high maternal transfer of ACIs and TXs groups in the maternal–fetal transmission of PIs (Li et al., 2019). Currently, humans can be exposed to PIs via many routes, including indoor dust ingestion and food intake; more data on the environmental occurrences, sources and exposure estimation are urgently needed to elucidate their environmental and health risks.

Electronic-waste (e-waste) recycling has been extensively identified as a main source for the emissions of many fugitive pollutants (Chen et al., 2018; Shen et al., 2019). China is a large processor of e-waste worldwide, and several e-waste recycling areas in South China are notoriously heavily contaminated areas for various organic pollutants. Generally, the concentrations of e-waste related pollutants in/near e-waste recycling sites are significantly higher than that in urban areas (Gu et al., 2010; Huang et al., 2013). PI-containing consumables, including adhesives, coatings, UV-cured ink and other light-sensitive materials (Ibrahim et al., 2013; Matsubara and Ohtani, 2007; Williams et al., 2000), are broadly and largely applied in electronic products and equipment such as crystalline semiconductors and laser printers (Jung et al., 2013; Malik et al., 2015; Stanculescu et al., 2006). Obviously, when these electronic items are being discarded, e-waste recycling area will be the ultimate disposal place for them. Considering the more frequent replacement and shorter lifecycle of current electronic products, the contamination of PIs in typical e-waste recycling area and potential influences of transportation on surrounding environments deserve special attention.

In this study, a typically mega e-waste recycling industrial park and its adjacent residential communities were selected as a case study region. A broad range of PIs, including BZPs, TXs, ACIs, and POs, were included in a comprehensive analysis to address the abovementioned concern. Indoor dust samples were collected from e-waste recycling facilities and adjacent residential homes; further, dust samples from urban homes far away from e-waste recycling activities were also collected as control samples for comparison. The aims of this work are to uncover the current pollution status, including the occurrence, concentrations, and composition profiles of PIs in an e-waste recycling area and to provide a comparative analysis of human exposure to these emerging toxic chemicals through dust ingestion between heavily contaminated and general indoor environments.

2. Material and methods

2.1. Background on the study area

The selected study area (N 23.5°, E 113.0°) covers a typical mega e-waste recycling industrial park and its adjacent residential communities and is located in Shijiao Town, Qingyuan City, Guangdong Province in South China. Shijiao Town is a well-known e-waste recycling area with the most intensive dismantling activity in South China. The central urban area of Guangzhou City, covering three typical urban residential communities, was selected for comparative study. Guangzhou City is the provincial capital of Guangdong Province, which is ~80 km away

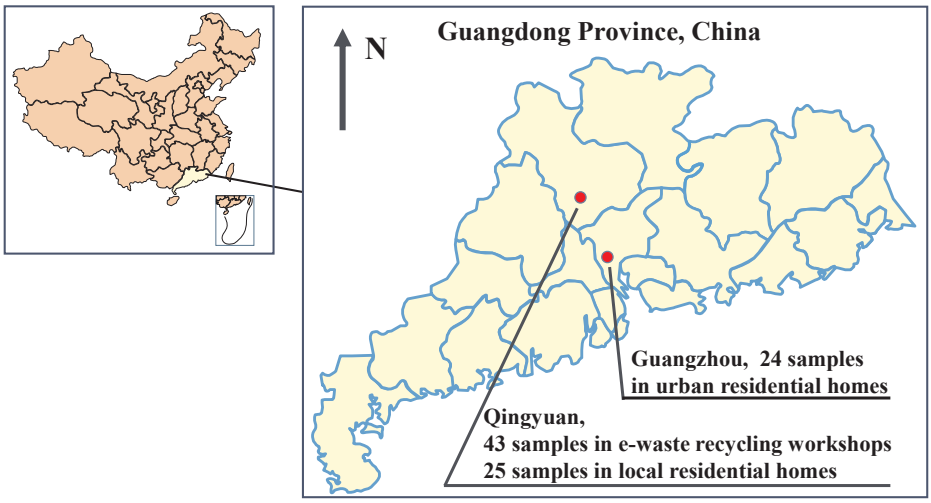

Fig. 1. Sampling locations of two cities located in Guangdong Province, South China.

from the e-waste recycling site. The sampling information is shown in Fig. 1. More detailed information regarding the background of the study region and the sampling map can be found in our previous studies (Chen et al., 2018; Shen et al., 2019).

2.2. Field sample collection

Dust samples were collected from the research and control areas between September 2016 and July 2017. A commercial vacuum cleaner attached with a customized, precleaned paper bag was used for dust sample collection. Floor dust was collected from each e-waste workshop, and only one pooled dust sample was collected from each e-waste workshop. Finally, 43 indoor dust samples were obtained from the workshops in the e-waste recycling industrial park. A total of 25 local homes from adjacent communities around the industrial park (within ~4 km) were recruited, and 25 dust samples were collected from these local homes. Only a composite sample composed of floor dust and elevated surface dust from house furnishings and appliances was collected from each local home. In addition, 24 urban homes located in the central urban area of Guangzhou City were recruited, which were equipped with essential household electrical appliances with no upgrading or replacement in the last few years. Similar to the sampling method for local home dust, 24 urban home dust samples were collected as the control samples. It should be noted that, dust from e-waste workshops may be mostly composed of soil and fine particulates from e-waste raw materials whereas those from homes may include many debris and air particulate matter besides soil. After collection, the paper collection bags were wrapped with precleaned aluminum foil. Six field blanks in three kinds of indoor environments were prepared using precleaned sodium sulfate. The samples were dried naturally to remove moisture and then sieved through a 100 μm stainless sieve prior to storage at −20 °C in amber glass jars until chemical analysis.

2.3. Standards and reagents

Four classes of 25 PIs, including 9 BZPs, 8 ACIs, 4 TXs, and 4 POs, were included in this study. The structure and CAS numbers of the 25 PIs are shown in Fig. S1 and Table S1. Nine BZPs, namely, BP, 4-methylbezophenone (4-MBP), PI-184, 4-phenylbenzophenone (PBZ), 1,2-diphenyl-1,2-ethanedione (Benzil), 2-ethylanthraquinone (EAQ), MBB, PI-651 and 4-methyl-4′-benzoyldiphenyl sulfide (MBPPS); eight ACIs, namely, 4-(dimethylamino) benzophenone (DMAB), MK, 4,4′-bis(diethylamino) benzophenone (Michler's ethylketone, MEK), PI-907, ethyl-4-aminobenzoate (EAB), EDMAB, EHDAB and 2-benzyl-2-(dimethylamino)-4′-morpholinobutyrophenone (PI-369); four TXs, namely, thioxanthone (TX), 2-chlorothioxanthone (2-Cl-TX), 2-ITX and DETX; and four POs, namely, triphenylphosphine oxide (TPPO), TPO, ethylphenyl (2,4,6-trimethylbenzoyl) phosphinate (TPO-L), and phenylbis (2,4,6-trimethylbenzoyl) phosphine oxide (PI-819)) were obtained from TCI Inc. (Tokyo, Japan). Two isotopically labeled internal standards (IS), $^{13}C_4$-benzophenone ($^{13}C_4$-BP) and 2-isopropyl-d7-thioxanthone (2-ITX-d7), were purchased from Sigma-Aldrich (St. Louis, MO, USA). Triphenyl phosphate-d15 (TPHP-d15) was purchased from Cambridge Isotope Laboratories, Inc. (Andover, MA). Methanol (MeOH) and acetonitrile (ACN) were of HPLC grade and obtained from Merck (Darmstadt, Germany). Ultra-pure water was prepared using a Milli-Q® Integral system (Millipore, USA). Commercial SPE cartridges (Oasis prime HLB, 60 mg/3.0 mL) were supplied by Waters (Milford, MA, USA).

2.4. Sample preparation and instrumental analysis

Sample extraction and cleanup were according to the previous studies with minor modifications (Liu et al., 2015; Liu and Mabury, 2019a). Briefly, a 50 mg dust sample was spiked with $^{13}C_4$-BP, 2-ITX-d7, and TPHP-d15 (10 ng each) and transferred into a 10 mL glass tube. After equilibration for 2 h, 5 mL of MeOH were added to each dust sample. The sample was shaken for 30 min, and then ultrasonically extracted for another 30 min. The mixtures were centrifuged at 4,500 rpm for 15 min, and the supernatant was transferred into clean glassware. The same extraction operation was repeated three times and the extracts combined. The combined extracts were concentrated to near dryness under a stream of nitrogen, and the solvent was exchanged into 4 mL ACN. Further cleanup was conducted with an Oasis prime HLB cartridge. The extract was passed through the cartridge with a flow rate of one drop per second. The target PIs were eluted with 6 mL ACN/MeOH (v/v = 9:1). The eluate was concentrated under a gentle nitrogen stream to near dryness, and reconstituted in 1 mL of MeOH. Finally, each purified dust sample extract was filtered through a filter membrane (GHP, 0.22 μm, Waters, USA) before instrumental analysis.

Instrumental analysis for PIs was based on our previous work (Li et al., 2019) and previous studies (Liu et al., 2015; Liu and Mabury, 2019a). The target compounds were analyzed using an electrospray triple quadrupole mass spectrometer (5500, AB SCIEX Redwood City, CA, USA) connected with a high-performance liquid chromatography (Shimadzu Corporation Inc., Kyoto). Electrospray ionization (ESI) was operated in the positive mode. Precursor and product ion combinations specific to each analyte were monitored in multiple reaction-monitoring (MRM) mode. Concentrations of target PIs were quantified with an isotope-diluted method. The detailed information on the MRM transitions of individual target compounds and their optimized MS/MS parameters are given in Table S2 in the Supplementary material.

2.5. Quality assurance and quality control

Each analytical batch of ten samples included two procedural blanks (sodium sulfate instead of dust) and two matrix-spiked samples (spiked concentrations of 10 and 100 ng/g). As shown in Table S3, the average recoveries of the target compounds in the spiked matrix were 84–115%, and the relative standard deviations varied from 2.9 to 12.7%. Randomly selected six extracts of dust samples were fortified with known concentrations of PIs for determining the matrix effect (ME). The average MEs for individual PIs were between 89 and 107% (Table S3), indicating no significant ionization suppression/enhancement for the analytes in dust. The quantitative methods were validated by examining the accuracy and precision. For accuracy, the deviations of IS-corrected quantitative results from the known values were ≤ 15%. For precision, the relative standard deviations (RSDs) in duplicate sample tests were ≤ 10%. The method detection limits (MDLs) were defined as the concentrations corresponding to a signal-to-noise ratio of three and were in the range of 0.03–1.5 ng/g. Trace levels of BP (1.85 ± 0.47 ng/g) and PI-184 (1.56 ± 0.24 ng/g) were detected in procedural blanks but contributed to < 10% of the average concentrations in the same batch of samples, and the reported concentrations for the two compounds were subtracted from the blank values. The levels of the field blanks were similar to those of the procedural blanks, thus indicating that no contamination occurred during sample collection. A nine-point calibration curve with concentrations in the range of 0.01–100 ng/mL was prepared for the quantification of target PIs, and the regression coefficient (r^2) of each calibration curve was > 0.995.

2.6. Calculation of daily intake

The estimated daily intake (EDI, ng/kg bw/day) of PIs via dust ingestion was calculated according to the following equation (Liu and Mabury, 2019a):

$$EDI = (C \times DIR)/BW \quad (1)$$

where "C" is the concentration of target analyte, "DIR" is the dust ingestion rate (g/day) and "BW" is the body weight (kg). In this study, we obtained the exposure factors from The Exposure Factors Handbook of the Chinese Population (EFHC) (Duan, 2015), which provided Chinese

human exposure factors of different regions, ages, and genders. Detailed information about the body weight and DIR for the general adults (19–70 years) and occupation workers (19–70 years) are found in Table S4.

Monte Carlo simulation was used to perform quantitative uncertainty analysis (Metropolis and Ulam, 1949; Thompson and Graham, 1996), employing as inputs probability distributions on the basis of empirical data. In this study, Monte Carlo simulation was utilized to estimate the values of EDIs for the general adults and occupation workers. In brief, the propagation of uncertainty through the Eq. (1) was simulated. Statistical distributions were derived for PI compound concentration, DIR and BW. The nonparametric Kolmogorov-Smirnov test ($\alpha = 0.01$) was used to compare each empirical statistical distribution with the sample probability distribution. The statistical distributions were tested by batch fit modules, and the normal, lognormal and Weibull distributions were included (Kretzschmar and Apt, 1977; Peng et al., 2016). This simulation was performed in Crystal Ball© (Oracle, Redwood City, CA, USA) and was set at 20,000 trials. Detailed information about the statistical distribution types and their corresponding parameter values are shown in Table S4.

2.7. Statistical analysis

Date statistical analysis was performed using SPSS software version 19.0, and the significant level was accepted when $p < 0.05$. Detection frequency (DF), geometric mean (GM), median, mean and range were adopted for descriptive statistics of PI concentrations. Concentrations below the MDLs were replaced by values equal to half of the MDLs for statistical analysis. Nonparametric tests (Kruskal-Wallis-H and Mann-Whitney-U) were used to identify the significant difference in concentrations between different sample types and between different PI groups. Spearman's test (two-tailed) was used to examine correlations among the analyte levels.

3. Results and discussion

3.1. Concentrations of four classes of emerging PIs identified in e-waste dust, local home dust, and urban home dust

Descriptive statistics of the concentrations of four classes of PIs (BZPs, ACIs, TXs, and POs) in e-waste dust, local home dust, and urban home dust samples are summarized in Table 1. All 25 target PIs were detected in e-waste dust, and 17 of the 25 target PIs were detected in local home dust. Comparatively, 15 of the 25 target PIs were identified in urban home dust. The total concentrations of PIs (ΣPIs) in e-waste dust ranged from 186–7290 ng/g (GM of 1290 ng/g), and the wide variation of ΣPIs may be attributed to different types of e-waste recycled at these workshops. The ΣPIs in e-waste dust were significantly higher than those in adjacent home dust (67.3–633 ng/g, GM of 221 ng/g) ($p < 0.01$) but were comparable to the measured values in urban home dust (447–8270 ng/g, GM of 1310 ng/g). The results indicate ubiquitous occurrences of multiple classes of PIs in various indoor environments. The measured ΣPIs in indoor dust from urban homes in China are similar to the reported levels in Canada (GM of 1480 ng/g) (Liu and Mabury, 2019a). PIs are reported to be widely used as chemical additives in food packaging materials and other household products (Liu and Mabury, 2019a). The frequent use of PI-containing household products may be the main influence factor on the elevated levels of PIs in urban home dust. Detailed box-whisker-plots of the concentration distributions of BZPs, ACIs, TXs, and POs in three types of indoor dust are illustrated in Fig. 2. BZPs and POs were two dominant groups in all the dust samples, which showed significantly higher levels than those of ACIs and TXs ($p < 0.01$). Furthermore, we find that the dust concentrations of ACIs and TXs in e-waste recycling facilities were significantly higher than those in adjacent communities and urban houses, but this was not the case for BZPs and POs. This finding suggests that more emissions of ACIs and TXs take place in the e-waste recycling area, while other BZP and PO sources from nonelectronic consumables are present in the household environment.

Benzophenones. All nine BZPs were detected in e-waste and local home dust samples, while eight of the nine target BZPs were detected in urban home dust samples. All nine BZPs, except MBPPS, were detected with high frequencies (77–100%). In e-waste dust, the most abundant congeners were identified as: benzil (GM: 206 ng/g) > BP (GM: 87.2 ng/g) > EAQ (GM: 40.9 ng/g) > PI-184 (GM: 33.6 ng/g). Benzil exhibited much higher concentrations than other detectable BZPs. In local home dust, the top four congeners in this family were identified as: BP (GM: 29.8 ng/g) > benzil (GM: 26.9 ng/g) > PI-184 (GM: 15.6 ng/g) > EAQ (GM: 11.7 ng/g). BP exhibited a slightly higher level than benzil but was approximately 2 or 3 times higher than PI-184 and EAQ. In the e-waste recycling facilities and adjacent communities, although the same four dominant congeners of BZPs were identified, their relative contributions to the total concentration of BZPs (ΣBZPs) between the two sampling locations were obviously different. The finding suggested that dust sources of BZPs in local residential homes might be not only from transport from near e-waste dust but also from the emission of nonelectronic household consumer products. The combined results led to a BZP composition profile in local home dust different from that in e-waste dust (Fig. 3). For further comparison, BZPs were analyzed in typical urban home dust samples, and the dominant congeners were identified in turn as: BP (GM: 341 ng/g) > benzil (GM: 59.0 ng/g) > PBZ (GM: 34.7 ng/g) > PI-184 (GM: 22.3 ng/g). Apparently, BP was the most abundant congener in urban home dust, with a much higher level than that of other BZPs, which was consistent with a previous report in indoor dust in Canada (Liu and Mabury, 2019a). The BZP composition profile in urban home dust was significantly different from that identified in e-waste and local home dust, suggesting that multiple sources existed in urban household environments.

By comparing the concentrations of individual BZPs in dust samples from the three locations, we found that all nine BZPs, except PBZ, exhibited significantly higher concentrations in e-waste dust than local home dust ($p < 0.001$), indicating that e-waste dismantling activities contributed to the high residues of BZPs in indoor dust. Moreover, the concentrations of benzil and EAQ in e-waste dust were significantly higher than those in urban home dust ($p < 0.001$), but the concentrations of BP and PBZ in urban home dust were significantly higher than those in e-waste dust ($p < 0.001$). These comparisons indicate that more emissions of benzil and EAQ may occur during e-waste recycling, while more emissions of BP and PBZ may be present in consumption of nonelectronic products in urban household environments. In fact, benzil was reported to be used in large quantity as polymer intermediates in adhesives (Abd-Alla, 1991), and it was also used in crystalline semiconductors/films for electronic application (Stanculescu et al., 2004, 2006). In addition, benzil is a photodegradation product of PI-651 (Liu and Mabury, 2019a). This can explain the high residues of benzil in e-waste dust. As for BP, in addition to being a photoinitiator, it is also widely used as UV absorber, fragrance enhancer, and as an additive in plastics, coatings, adhesives and personal care products (Kawamura et al., 2003; Liao and Kannan, 2014). Thus, higher concentrations of BP in urban home dust are mainly attributed to daily frequent use of various BP-containing products. Based on the summary results (Table 1), the ΣBZPs in e-waste dust were comparable to or even lower than those in urban home dust due to large contributions of BP and PBZ from nonelectronic household products. In addition, the ΣBZPs in local home dust were significantly lower than those in urban home dust, which may be attributed to more use of BZP-containing products in general urban families than in locally rural homes (Wang et al., 2013).

Amine coinitiators. All eight ACIs were detected in e-waste dust samples, while only four and three of the eight target ACIs were detected in local and urban home dust samples, respectively, indicating

Table 1
Descriptive statistics of measured concentrations (ng/g) of four classes of emerging PIs in indoor dust samples.

Compound	**E-waste recycling workshops (n = 43)**					**Local residential homes (n = 25)**					**Urban residential homes (n = 24)**				
	N > MDL(%)	GM	Median	Mean	Range	N > MDL(%)	GM	Median	Mean	Range	N > MDL(%)	GM	Median	Mean	Range
BP	43(100)	87.2	80.7	143	10.2–1030	25(100)	29.8	27.2	46.6	9.20–402	24(100)	341	490	562	1.41–1260
Benzil	43(100)	206	167	653	17.8–5770	25(100)	26.9	27.2	35.1	3.00–119	24(100)	59.0	58.9	71.2	21.8–170
PI-184	43(100)	33.6	26.5	44.7	8.64–196	25(100)	15.6	16.1	16.7	7.09–30.1	23(96)	22.3	21.0	45.2	< MDL–191
4-MBP	43(100)	22.8	19.8	41.6	3.18–298	25(100)	9.09	8.14	14.7	3.97–128	16(75)	2.80	6.14	7.59	< MDL–57.7
EAQ	43(100)	40.9	33.1	71.9	11.3–606	25(100)	11.7	11.7	12.0	7.90–18.8	11(46)	1.54	< MDL	3.86	< MDL–20.7
PBZ	43(100)	5.25	4.20	7.52	1.34–48.7	25(100)	5.73	5.93	7.76	1.32–34.2	24(100)	34.7	23.5	150	5.06–2290
PI-651	43(100)	15.8	23.3	45.2	0.14–325	10(40)	0.17	< MDL	1.25	< MDL–5.75	22(92)	7.42	12.2	16.9	< MDL–136
MBPPS	16(37)	0.17	< MDL	2.62	< MDL–33.9	1(4)	0.03	< MDL	0.07	< MDL–1.14	0(0)	< MDL	< MDL	< MDL	< MDL
MBB	33(77)	3.08	4.45	13.0	< MDL–155	21(84)	2.79	3.83	6.32	< MDL–38.6	21(88)	12.1	20.5	31.1	< MDL–93.4
ΣBZPs		600	639	1022	80.7–6460		121	114	140	55.7–488		710	754	888	162–2970
MK	2(5)	0.04	< MDL	0.33	< MDL–10.3	7(28)	0.19	< MDL	18.1	< MDL–272	0(0)	< MDL	< MDL	< MDL	< MDL
MEK	5(12)	0.08	< MDL	9.57	< MDL–351	0(0)	< MDL	< MDL	< MDL	< MDL	0(0)	< MDL	< MDL	< MDL	< MDL
EDMAB	3(9)	0.05	< MDL	1.08	< MDL–38.1	0(0)	< MDL	< MDL	< MDL	< MDL	9(38)	0.12	< MDL	1.42	< MDL–23.7
EHDAB	2(5)	0.05	< MDL	0.12	< MDL–2.08	0(0)	< MDL	< MDL	< MDL	< MDL	0(0)	< MDL	< MDL	< MDL	< MDL
PI-369	9(21)	0.14	< MDL	0.93	< MDL–14.4	3(12)	0.09	< MDL	0.42	< MDL–7.75	0(0)	< MDL	< MDL	< MDL	< MDL
PI-907	39(91)	9.83	11.8	75.8	< MDL–653	12(48)	0.37	< MDL	4.38	< MDL–28.5	2(8)	0.05	< MDL	1.74	< MDL–35.2
DMAB	6(14)	0.07	< MDL	4.36	< MDL–131	0(0)	< MDL	< MDL	< MDL	< MDL	0(0)	< MDL	< MDL	< MDL	< MDL
EAB	41(95)	14.8	17.2	76.7	< MDL–1960	6(24)	0.07	< MDL	0.68	< MDL–12.6	7(29)	0.11	< MDL	4.45	< MDL–54.1
ΣACIs		47.5	49.1	169	< MDL–2290		3.31	4.18	23.7	< MDL–272		1.67	1.15	7.86	< MDL–55.1
TX	11(26)	0.39	< MDL	4.59	< MDL–59.4	0(0)	< MDL	< MDL	< MDL	< MDL	0(0)	< MDL	< MDL	< MDL	< MDL
2-ITX	42(98)	19.5	18.1	55.2	< MDL–928	24(96)	3.45	4.94	7.23	< MDL–32.3	18(75)	2.06	5.15	7.12	< MDL–22.2
DETX	42(98)	9.22	10.9	25.6	< MDL–424	10(40)	0.14	< MDL	0.66	< MDL–3.22	22(92)	6.68	10.4	96.2	< MDL–1990
2-Cl-TX	1(2)	0.03	< MDL	0.19	< MDL–6.86	0(0)	< MDL	< MDL	< MDL	< MDL	0(0)	< MDL	< MDL	< MDL	< MDL
ΣTXs		35.1	36.3	85.6	2.84–1350		4.79	5.27	8.07	< MDL–32.5		13.9	19.3	104	1.48–1995
TPPO	43(100)	380	421	609	32.1–2618	25(100)	62.7	75.5	77.4	8.64–239	24(100)	376	357	604	91.8–4980
TPO	7(16)	2.34	< MDL	5.23	< MDL–41.5	1(4)	1.65	< MDL	2.16	< MDL–18.1	6(25)	8.16	< MDL	45.8	< MDL–301
TPO-L	1(2)	0.53	< MDL	0.59	< MDL–4.33	0(0)	< MDL	< MDL	< MDL	< MDL	0(0)	< MDL	< MDL	< MDL	< MDL
PI-819	3(7)	0.41	< MDL	0.68	< MDL–11.5	0(0)	< MDL	< MDL	< MDL	< MDL	0(0)	< MDL	< MDL	< MDL	< MDL
ΣPOs		389	425	615	34.4–2620		66.0	77.8	80.4	11.0–241		420	380	652	96.5–5290
ΣPIs		1290	1420	1890	186–7290		221	213	253	67.3–633		1310	1180	1652	447–8270

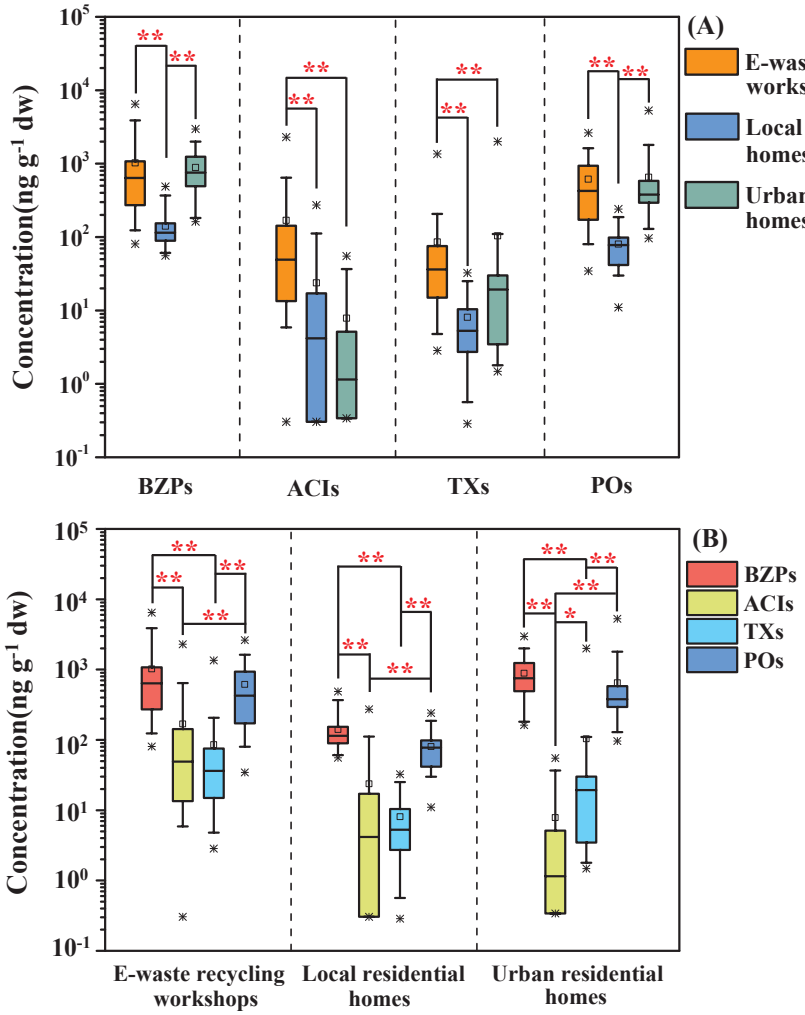

Fig. 2. Box-whisker-plots of concentration distributions of BZPs, ACIs, TXs and POs in indoor dust collected from three locations. The plots were categorized to illustrate by sampling locations (A) and PI groups (B). The box corresponds to the interquartile range with the lower and upper edges designating the 25th and 75th percentiles, respectively. The horizontal line indicates the median concentration. The whiskers represent 5th and 95th percentiles. □ and *represent the mean and maximum/minimum values, respectively. One and two red * indicate significance at the level $p < 0.05$ and $p < 0.01$, respectively. (For interpretation of the references to colour in this figure legend, the reader is referred to the web version of this article.)

the release of a broad spectrum of ACIs into indoor dust due to e-waste dismantling/recycling activities. The total concentration of ACIs (ΣACIs) in e-waste dust ranged from < MDL–2290 ng/g with a GM of 47.5 ng/g, which was more than one order of magnitude higher than in local home dust (GM: 3.31 ng/g) and urban home dust (GM: 1.67 ng/g), indicating that e-waste dismantling activities also contributed to the relatively high residues of ACIs in indoor dust. EAB and PI-907 were detected in over 90% of the e-waste dust samples with the relatively highest GMs of 14.8 and 9.83 ng/g, respectively. Thus, EAB and PI-907 were identified as the main contributors to ΣACIs during the e-waste dismantling/recycling. Low concentrations of four ACIs (MK, PI-369, PI-907, and EAB) were detected at DF < 50% in local home dust, but no dominant ACI congener was found. Only three ACIs, namely, EAB, PI-907 and EDMAB, were identified at low DF in urban home dust, and their concentrations were substantially lower than previously reported levels in household dust from North China and Canada (Liu et al., 2015; Liu and Mabury, 2019a). The results indicated that ACIs' usage pattern or release mode might vary in different counties/regions. Since the distribution pattern of ACIs in local home dust was roughly similar to that in urban home dust, but significantly different from that in e-waste dust, we infer that ACIs (Log K_{oa} from 7.41 for EDMAB to 14.6 for PI-369) (Table S1) may be less transportable regionally via dust deposition due to their relatively low volatility.

Thioxanthones. All four TXs were detected in e-waste dust, and 2-ITX and DETX were identified as the dominant congeners with relative high concentrations detected in almost all e-waste dust samples. Low concentrations of 2-ITX and DETX were widely detected in local home dust and urban home dust samples, but no other TX congeners (TX and 2-Cl-TX) were identified in the home dust samples. In a previous study, 2-ITX and DETX were also identified as the most abundant congeners in indoor dust in Canada (Liu and Mabury, 2019a). Given that 2-ITX and DETX have strong endocrine-disrupting activities (Peijnenburg et al., 2010; Reitsma et al., 2012), the widespread occurrence of the two emerging chemicals in indoor environments should raise concern. The total concentration of TXs (ΣTXs) in e-waste dust ranged from 2.84 to 1350 ng/g with a GM of 35.1 ng/g, substantially higher that in local home dust (4.79 ng/g) and urban home dust (13.9 ng/g), thus indicating that e-waste dismantling activities are responsible for the relatively high residues of TXs in indoor dust. Based on these results, 2-ITX and DETX may be in wide use in electronic products and/or plastic packing materials.

Phosphine oxides. All four POs (TPPO, TPO, TPO-L, and PI-819) were detected in e-waste dust, and only two POs (TPPO and TPO) were detected in local and urban home dust. TPPO was detected in all dust samples and was easily identified as the most abundant PO congener with elevated concentrations, but in contrast, the three other POs were only detected occasionally with very low levels. Concentrations of TPPO exceeded by two orders of magnitude those of other detectable POs in indoor dust. TPPO concentrations in e-waste dust ranged from 32.1 to 2618 ng/g with a GM of 380 ng/g; these values were comparable to those in urban home dust (91.8–4980 ng/g with a GM of 376 ng/g) but were significantly higher than those in local home dust (8.64–239 ng/g with a GM of 62.7 ng/g). In a previous study, TPPO was also identified as the predominant PO congener in indoor dust in

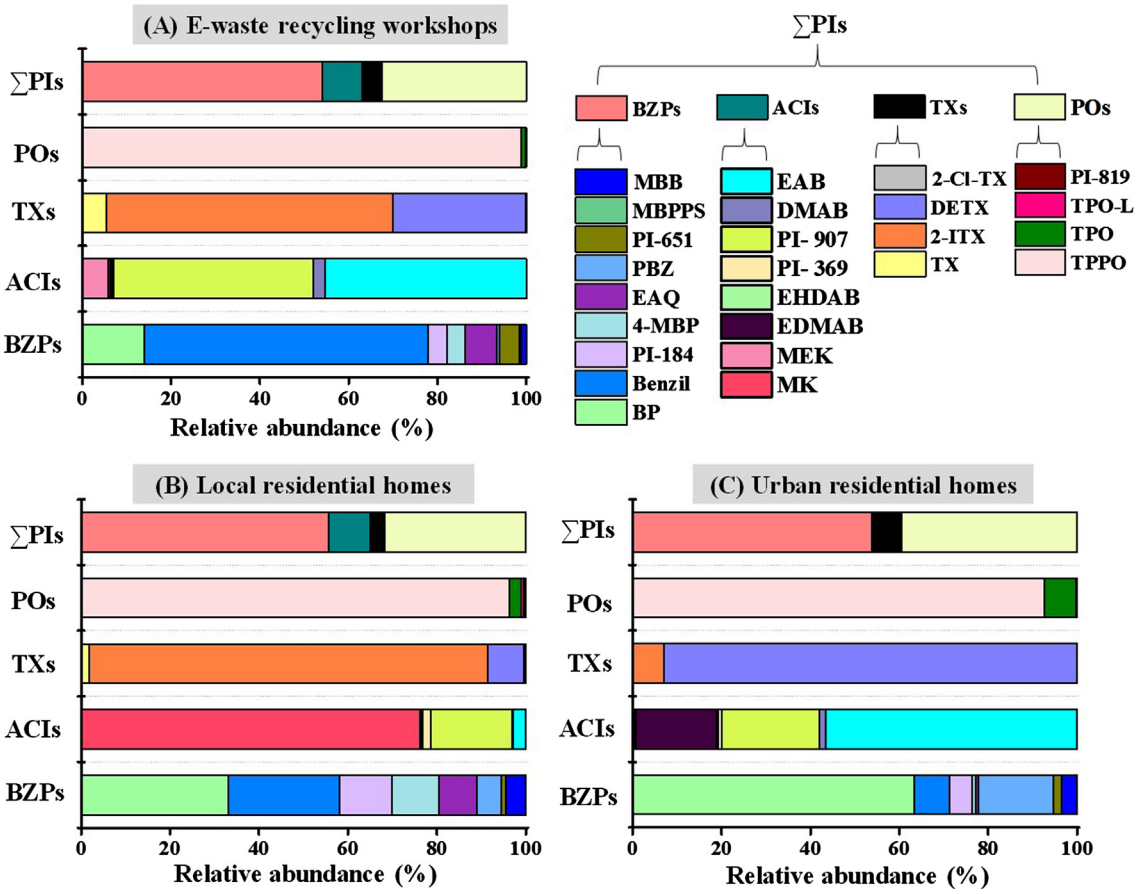

Fig. 3. Characteristic composition profiles of ΣPIs and individual PI groups in three types of indoor dust samples from (A) e-waste recycling workshops; (B) local residential homes and (C) urban residential homes.

Canada (Liu and Mabury, 2019a). Here, the GM or median concentrations of TPPO measured in e-waste dust and urban home dust were approximately two times higher than the reported levels in Canada.

It has been reported that TPPO was frequently used as photoinitiator in food packaging materials (Liu and Mabury, 2019a). In addition to being a photoinitiator, TPPOs, along with organophosphate esters, are widely used as novel flame retardants in a wide range of consumer products in various indoor environments, including homes, offices, conference halls and laboratories (Faiz et al., 2016; Santín et al., 2016). Furthermore, environmental TPPO might derive from oxidation of triphenylphosphine, which is often used as an additive in biocides and lubricants (Liu and Mabury, 2019a). Thus, high levels of TPPO in e-waste dust may be attributed to its common use as photoinitiator and flame retardant in electronic products and frequent release during e-waste recycling; however, elevated TPPO levels in urban home dust may arise from the emissions of various household products other than electronic products. The much lower levels of TPPO in local home dust than urban home dust and e-waste dust suggest less use of TPPO-containing consumer products in these rural families and less diffusion of TPPO from e-waste source due to low volatility. The pollution levels of TPPO in indoor dust from e-waste workshops and urban homes were generally lower than the previously reported levels (1,010–13,600 ng/g) of two organophosphate esters (OPEs), namely, tris(1-chloro-2-propyl) phosphate (TCIPP) and tris(1,3-dichloro-2-propyl) phosphate (TDCIPP), but were comparable to or even higher than the levels of other individual OPEs (Guo et al., 2019). In spite of there being no available data regarding the toxic effects of TPPO, it still remains important to study the environmental occurrence and source of this new chemical, as it exhibited the highest concentration among all detected PIs in various environments and poses potentially unknown risks.

3.2. Characteristic composition profiles of PIs in indoor dust from the e-waste recycling area compared to the general urban homes

The composition profiles of ΣPIs and individual PI groups in three types of dust samples are shown in Fig. 3. The characteristic composition profile of PIs in dust from e-waste workshops and adjacent local homes were identified by comparison with that from urban homes. Overall, for individual PIs, TPPO, BP, and benzil were the top three compounds. With the exception of TPPO, the second highest abundance of a PI congener was characterized by benzil in e-waste dust but by BP in urban home dust, thus indicating that e-waste dismantling/recycling caused more emissions of TPPO and benzil. For PI groups, ΣPIs in all dust samples were dominated by BZPs and POs that jointly accounted for more than 80% of ΣPIs; however, after BZPs and POs, ACIs contributed much higher abundance of ΣPIs in e-waste dust and local home dust than in urban home dust, suggesting that the release from electronic products was the main source of ACIs in the indoor environments.

The composition profile of BZPs was dominated by benzil, 4-MBP and EAQ in e-waste dust, which was clearly different from the profile of BZPs dominated by BP and PBZ in urban home dust. The composition profile of ACIs was characterized by EAB, PI-907 and MEK in e-waste dust, which still remained somewhat different from the profile of ACIs characterized by EAB, PI-907 and EDMAB in urban home dust. The composition profile of the TXs was dominated by more abundant 2-ITX in e-waste dust and local home dust, which was significantly different from the profile of TXs dominated by more abundant DETX in urban home dust. Unlike BZPs, ACIs, and TXs, POs exhibited a similar composition profile in all dust samples. Based on these results, we concluded that, apart from POs, the e-waste dismantling/recycling

Table 2
Spearman's correlation matrix of the frequently detected PIs in indoor dust samples from e-waste recycling facilities (n = 43; PI congeners with detection frequency < 50% were not included for analysis).

	BP	Benzil	PI-184	4-MBP	EAQ	PBZ	PI-651	MBB	PI-907	EAB	2-ITX	DETX
Benzil	0.552**											
PI-184	0.552**	0.144										
4-MBP	0.584**	0.429**	0.740**									
EAQ	0.407**	−0.290	0.450**	0.322*								
PBZ	0.541**	0.122	0.599**	0.565**	0.647**							
PI-651	0.494**	0.555**	0.681**	0.859**	0.260	0.444**						
MBB	0.565**	0.425**	0.725**	0.676**	0.412**	0.543**	0.731**					
PI-907	0.298	−0.136	0.563**	0.456**	0.413**	0.538**	0.408**	0.349*				
EAB	0.443**	−0.186	0.431**	0.319*	0.576**	0.450**	0.308*	0.413**	0.357*			
2-ITX	0.330*	−0.262	0.592**	0.419**	0.714**	0.687**	0.315*	0.496**	0.703**	0.545**		
DETX	0.404**	−0.113	0.544**	0.421**	0.733**	0.703**	0.396**	0.606**	0.583**	0.571**	0.797**	
TPPO	0.536**	0.149	0.518**	0.504**	0.214	0.296	0.567**	0.562**	0.349*	0.188	0.328*	0.350*

* Correlation is significant at the 0.05 level (two-tailed).
** Correlation is significant at the 0.01 level (two-tailed).

activities lead to characteristic emissions of multiple classes of PIs with relatively high levels in the environment.

3.3. Correlations analysis among the frequently detected PIs in indoor dust

Spearman's correlation matrices of the frequently detected PIs (DF > 50%) in indoor dust from the e-waste workshops, local homes and urban homes are shown in Tables 2, S5 and S6, respectively. In the e-waste dust, significant correlations (r = 0.308–0.797; p < 0.05) were identified among all 13 frequently detected PIs except for benzil, indicating their similar application in electronic products and common emission source from e-waste. In general, multiple PIs are combined for common use in photoinitiation (Neumann et al., 2009); thus, it can be expected that common releases of these PIs into indoor dust take place during the e-waste dismantling/recycling processes. Significantly different from the e-waste dust, only a fraction of significant correlations were observed between PIs in both local home dust (Table S5) and urban home dust (Table S6). The results indicated that multiple potential sources, including food packaging materials and other household products other than electronic products, were present in household environments (Liu and Mabury, 2019a). As we discussed above, most PIs may be less transported regionally from e-waste recycling workshops to local homes via dust deposition due to their relatively low volatility. Therefore, these influencing factors can explain the correlations between PIs in home dust different from those in e-waste dust.

3.4. Estimated daily intakes of PIs through dust ingestion for the e-waste dismantling workers and the general population

The EDIs of PIs via dust ingestion for the occupational e-waste workers, local adult residents, and urban adult residents were evaluated using Monte Carlo analysis under two exposure scenarios: median and high-end exposure. The median and high-end EDIs were calculated based on the median and 90th percentile (P90) concentrations in dust samples, respectively. The comparison of EDIs of four PI groups and ΣPIs via dust ingestion for the three representative populations are illustrated in Fig. 4. Detailed EDI values are given in Table S7. Specifically, the cumulative probability distributions of EDIs for the occupational workers in e-waste recycling facilities are shown in Fig. S2.

Under both of exposure scenarios, the EDI values generally decreased in the order of BZPs > POs > ACIs > TXs (Fig. 4) for the three populations. The median or high-end EDIs of BZPs and POs were approximately 1–2 orders of magnitude higher than those of ACIs and TXs for all exposed populations, indicating that the primary contributions to human dust exposure to PIs are from BZPs and TXs. The estimated median exposure of occupational e-waste workers to ΣPIs was 2.31 ng/kg bw/day, which was approximately 10 times higher than that for local adult residents and more than 2 times higher than that for urban adult residents. This suggests e-waste dismantling workers suffer from substantially high occupational exposure to PIs, which should be of concern. The high-end exposure to PIs showed a similar exposure mode as that of the median exposure, and likewise, the EDIs of BZPs and POs were much higher than those of ACIs and TXs. The estimated high-end exposure to ΣPIs was as high as 7.72 ng/kg bw/day for occupational workers, which was nearly 20 and 3 times higher than that of local and urban adult residents, respectively, further implying potentially high PI exposure risk posed to e-waste dismantling workers. Moreover, compared with the two exposure scenarios, the high-end exposure levels to PIs exceeded by 2–7 times the corresponding median exposure levels.

As newly identified emerging contaminants, toxicological studies concerning PIs are very limited. To our knowledge, BP is the only PI congener that can be currently assessed for the health risk using the hazard quotient (HQ) based on a proposed reference dose (RfD) of 30 μg/kg bw/day. Due to a serious lack of RfDs for PIs, risk assessments cannot be accurately obtained at present for these new chemical contaminants. If compared only with the available RfD mentioned above, the calculated EDI of BP or ΣPIs via dust ingestion, even in the case of a high-end exposure scenario, was still much lower than the proposed RfD. Therefore, it appears that the current dust exposure to PIs would not cause any human health risks. However, it should be pointed out that, besides dust ingestion, food intake, air inhalation and dermal absorption may be equally important human exposure routes to PIs. Consequently, the health risks could be substantially underestimated here due to no combination of other EDI values from other exposure routes. Moreover, as discussed in our recent works (Shen et al., 2019), dust from an e-waste recycling area has been proved as a large accumulation of many conventional toxic organic pollutants in addition to these newly identified chemicals. Therefore, given the multicomponent chemical 'cocktail' effects, the potential combined risks from previously known conventional contaminants and newly identified emerging contaminates should not be overlooked. With increasing emerging contaminants being continuously identified in e-waste recycling areas, our results here highlight the potential severe synergistic risks from the combined exposure to novel and conventional contaminants, which should receive greater attention. More investigations on other human exposure routes to PIs and on the individual and combined toxicological effects of PIs are strongly recommended to be performed in the future.

3.5. Conclusion

This study has demonstrated that multiple classes of emerging PIs are ubiquitous and prevalent in e-waste recycling areas, with particularly high levels of most PIs in e-waste dust. Characteristic composition

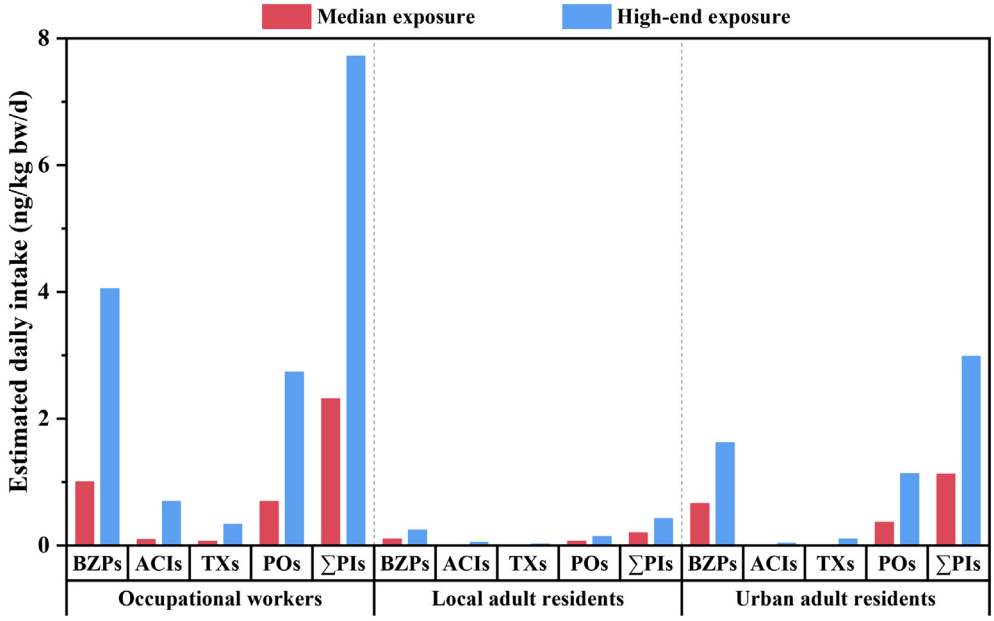

Fig. 4. Estimated daily intakes of BZPs, ACIs, TXs, POs, and ΣPIs via indoor dust ingestion for occupational workers of e-waste dismantling, local adult residents living in e-waste recycling area, and urban adult residents under median and high-end exposure scenarios.

profiles of PIs in indoor dust from the e-waste recycling area were observed compared to those in the control samples from general urban homes. Significant correlations were positively identified among almost all the frequently detected PIs in e-waste dust. The results reveal that e-waste dismantling/recycling activities result in largely common releases of a wide range of PIs. The estimated daily intakes of PIs via dust ingestion for the e-waste dismantling workers were several times higher than those for both local adult and general urban adult residents. In view of potential carcinogenicity and other unknown side effects of most PIs, further investigations are warranted to advance a variety of fields, including investigations the environmental occurrence, behavior, human exposure, and toxicity of these emerging chemicals.

Declaration of Competing Interest

The authors declare that they have no known competing financial interests or personal relationships that could have appeared to influence the work reported in this paper.

Acknowledgements

This work was supported by the National Natural Science Foundation (Nos. 21577142, 21876063, 41522304, 21607057, 41701544), the Guangdong (China) Innovative and Entrepreneurial Research Team Program (No. 2016ZT06N258), the China Postdoctoral Science Foundation (2019M653283), and Hubei Key Laboratory of Environmental and Health Effects of Persistent Toxic Substances, Jianghan University (PTS2019-09).

Appendix A. Supplementary material

Supplementary data to this article can be found online at https://doi.org/10.1016/j.envint.2020.105462.

References

Abd-Alla, M.A., 1991. Novel synthesis of poly (benzoin) and poly (benzil). Characterization and application as photosensitizer materials. Makromol. Chem. 192, 277–283.
Bradley, E.L., Stratton, J.S., Leak, J., Lister, L., Castle, L., 2013. Printing ink compounds in foods: UK survey results. Food. Addit. Contam. B. 6, 73–83.
Chen, H., Lam, J.C., Zhu, M., Wang, F., Zhou, W., Du, B., Zeng, L., Zeng, E.Y., 2018. Combined effects of dust and dietary exposure of occupational workers and local residents to short-and medium-chain chlorinated paraffins in a mega E-waste recycling industrial park in South China. Environ. Sci. Technol. 52, 11510–11519.
Council, E. European Council of the Paint, Printing Ink and Artists' Colours Industry. Exclusion list for printing inks and related products; 2006; http://www.foodcontactmaterials.com/materials/eupia.pdf.
Duan, X., 2015. Highlights of the Chinese Exposure Factors Handbook. Academic Press.
Faiz, Y., Wei, Z., Feng, J., Cheng, S., He, H., Zhu, J., 2016. Occurrence of triphenylphosphine oxide and other organophosphorus compounds in indoor air and settled dust of an institute building. Build. Environ. 106, 196–204.
Gallart-Ayala, H., Núñez, O., Lucci, P., 2013. Recent advances in LC-MS analysis of food-packaging contaminants. Trac. Trend. Anal. Chem. 42, 99–124.
Gallart-Ayala, H., Núñez, O., Moyano, E., Galceran, M.T., 2011. Analysis of UV ink photoinitiators in packaged food by fast liquid chromatography at sub-ambient temperature coupled to tandem mass spectrometry. J. Chromatogr. A. 1218, 459–466.
Gil-Vergara, A., Blasco, C., Picó, Y., 2007. Determination of 2-isopropyl thioxanthone and 2-ethylhexyl-4-dimethylaminobenzoate in milk: comparison of gas and liquid chromatography with mass spectrometry. Anal. Bioanal. Chem. 389, 605–617.
Gu, Z., Feng, J., Han, W., Wu, M., Fu, J., Sheng, G., 2010. Characteristics of organic matter in PM2. 5 from an e-waste dismantling area in Taizhou, China. Chemosphere 80, 800–806.
Guo, H., Zheng, X., Ru, S., Sun, R., Mai, B., 2019. Size-dependent concentrations and bioaccessibility of organophosphate esters (OPEs) in indoor dust: A comparative study from a megacity and an e-waste recycling site. Sci. Total. Environ. 650, 1954–1960.
Huang, D.-Y., Zhou, S.-G., Hong, W., Feng, W.-F., Tao, L., 2013. Pollution characteristics of volatile organic compounds, polycyclic aromatic hydrocarbons and phthalate esters emitted from plastic wastes recycling granulation plants in Xingtan Town, South China. Atoms. Environ. 71, 327–334.
Ibrahim, A., Stefano, L.D., Tarzi, O., Tar, H., Ley, C., Allonas, X., 2013. High-performance photoinitiating systems for free radical photopolymerization. Application to holographic recording. Photochem. Photobiol. 89, 1283–1290.
Japan. Japan Printing Ink Makers Association. Voluntary regulation concerning printing inks (negative list regulation); 2006; https://www.coatings.org.uk/Media/Download.aspx?MediaId=2106.
Jin, Z.Y., 2011. Adcance in photointiators. Image Technol. 23, 8–18.
Jung, T., Simat, T., Altkofer, W., Fügel, D., 2013. Survey on the occurrence of photoinitiators and amine synergists in cartonboard packaging on the German market and their migration into the packaged foodstuffs. Food. Addit. Contam. A. 30, 1993–2016.
Kawamura, Y., Ogawa, Y., Nishimura, T., Kikuchi, Y., Nishikawa, J.-I., Nishihara, T., Tanamoto, K., 2003. Estrogenic activities of UV stabilizers used in food contact plastics and benzophenone derivatives tested by the yeast two-hybrid assay. J. Health. Sci. 49, 205–212.
Kitchin, K.T., Brown, J.L., 1994. Dose-response relationship for rat liver DNA damage caused by 49 rodent carcinogens. Toxicology 88, 31–49.
Kretzschmar, J., Apt, K., 1977. Applicability of the Weibull distribution function to atmospheric radioactivity data; and Reply. Atoms. Environ. 11, 783–784.
Landuyt, K.L.V., Krifka, S., Hiller, K.A., Bolay, C., Waha, C., Meerbeek, B.V., Schmalz, G., Schweikl, H., 2015. Evaluation of cell responses toward adhesives with different photoinitiating systems. Dent. Mater. 31, 916–927.

Li, J., Lam, J.C.-W., Li, W., Du, B., Chen, H., Zeng, L., 2019. Occurrence and distribution of photoinitiator additives in paired maternal and cord plasma in a South China population. Environ. Sci. Technol. 53, 10969–10977.
Liao, C., Kannan, K., 2014. Widespread occurrence of benzophenone-type UV light filters in personal care products from China and the United States: an assessment of human exposure. Environ. Sci. Technol. 48, 4103–4109.
Liu, R., Lin, Y., Hu, F., Liu, R., Ruan, T., Jiang, G., 2015. Observation of emerging photoinitiator additives in household environment and sewage sludge in China. Environ. Sci. Technol. 50, 97–104.
Liu, R., Mabury, S.A., 2018. First detection of photoinitiators and metabolites in human sera from United States donors. Environ. Sci. Technol. 52, 10089–10096.
Liu, R., Mabury, S.A., 2019a. Identification of photoinitiators, including novel phosphine oxides, and their transformation products in food packaging materials and indoor dust in Canada. Environ. Sci. Technol. 53, 4109–4118.
Liu, R., Mabury, S.A., 2019b. Photoinitiators in breast milk from United States donors: occurrence and implications for exposure in infants. Environ. Sci. Technol. Lett. 6, 702–709.
Louis, G.M.B., Chen, Z., Kim, S., Sapra, K.J., Bae, J., Kannan, K., 2015. Urinary concentrations of benzophenone-type ultraviolet light filters and semen quality. Fertil. Steril. 104, 989–996.
Malik, H.H., Darwood, A.R., Shaunak, S., Kulatilake, P., Abdulrahman, A., Mulki, O., Baskaradas, A., 2015. Three-dimensional printing in surgery: a review of current surgical applications. J. Surg. Res. 199, 512–522.
Manojlovic, D., Dramićanin, M.D., Miletic, V., Mitić-Ćulafić, D., Jovanović, B., Nikolić, B., 2017. Cytotoxicity and genotoxicity of a low-shrinkage monomer and monoacylphosphine oxide photoinitiator: Comparative analyses of individual toxicity and combination effects in mixtures. Dent. Mater. 33, 454–466.
Matsubara, H., Ohtani, H., 2007. Rapid and sensitive determination of the conversion of UV-cured acrylic ester resins by pyrolysis-gas chromatography in the presence of an organic alkali. Anal. Sci. 23, 513–516.
Metropolis, N., Ulam, S., 1949. The Monte Carlo method. jJ-AM-STATASSOC, 44 (247): 335–341. September.
Morizane, M., Kawasaki, Y., Miura, T., Yagi, K., Esumi, S., Kitamura, Y., Sendo, T., 2015. Photoinitiator-initiated estrogenic activity in human breast cancer cell line MCF-7. J. Toxicol. Env. Heal. A. 78, 1450–1460.
Morohoshi, K., Yamamoto, H., Kamata, R., Shiraishi, F., Koda, T., Morita, M., 2005. Estrogenic activity of 37 components of commercial sunscreen lotions evaluated by in vitro assays. Toxicol. In. Vitro. 19, 457–469.
Network, I.B.F.A., 2005. Chronology of withdrawal of Nestle and other liquid milks.
Neumann, M.G., Schmitt, C.C., Horn Jr, M.A., 2009. The effect of the mixtures of photoinitiators in polymerization efficiencies. J. Appl. Polym. Sci. 112, 129–134.
Peijnenburg, A., Riethof-Poortman, J., Baykus, H., Portier, L., Bovee, T., Hoogenboom, R., 2010. AhR-agonistic, anti-androgenic, and anti-estrogenic potencies of 2-isopropylthioxanthone (ITX) as determined by in vitro bioassays and gene expression profiling. Toxicol. In. Vitro. 24, 1619–1628.
Peng, Q., Nunes, L.M., Greenfield, B.K., Dang, F., Zhong, H., 2016. Are Chinese consumers at risk due to exposure to metals in crayfish? A bioaccessibility-adjusted probabilistic risk assessment. Environ. Int. 88, 261–268.
Reitsma, M., Bovee, T.F., Peijnenburg, A.A., Hendriksen, P.J., Hoogenboom, R.L., Rijk, J.C., 2012. Endocrine-disrupting effects of thioxanthone photoinitiators. Toxicol. Sci. 132, 64–74.
Rhodes, M., Bucher, J., Peckham, J., Kissling, G., Hejtmancik, M., Chhabra, R., 2007. Carcinogenesis studies of benzophenone in rats and mice. Food. Chem. Toxicol. 45, 843–851.
Santín, G., Eljarrat, E., Barceló, D., 2016. Simultaneous determination of 16 organophosphorus flame retardants and plasticizers in fish by liquid chromatography-tandem mass spectrometry. J. Chromatogr. A. 1441, 34–43.
Shen, M., Ge, J., Lam, J.C., Zhu, M., Li, J., Zeng, L., 2019. Occurrence of two novel triazine-based flame retardants in an E-waste recycling area in South China: Implication for human exposure. Sci. Total. Environ. 683, 249–257.
Stanculescu, A., Antohe, S., Alexandru, H., Tugulea, L., Stanculescu, F., Socol, M., 2004. Effect of dopant on the intrinsic properties of some multifunctional aromatic compounds films for target applications. Synthetic. Met. 147, 215–220.
Stanculescu, A., Stanculescu, F., Alexandru, H., Socol, M., 2006. Doped aromatic derivatives wide-gap crystalline semiconductor structured layers for electronic application. Thin Solid Films 495, 389–393.
Thompson, K.M., Graham, J.D., 1996. Going beyond the single number: using probabilistic risk assessment to improve risk management. Hum. Ecol. Risk. Assess. A. Int. J. 2, 1008–1034.
Wang, L., Asimakopoulos, A.G., Moon, H.-B., Nakata, H., Kannan, K., 2013. Benzotriazole, benzothiazole, and benzophenone compounds in indoor dust from the United States and East Asian countries. Environ. Sci. Technol. 47, 4752–4759.
Williams, R.M., Khudyakov, I.V., Purvis, M.B., Overton, B.J., Turro, N.J., 2000. Direct and sensitized photolysis of phosphine oxide polymerization photoinitiators in the presence and absence of a model acrylate monomer: A time resolved EPR, cure monitor, and PhotoDSC study. J. Phys. Chem. B 104, 10437–10443.
Zhang, T., Sun, H., Qin, X., Wu, Q., Zhang, Y., Ma, J., Kannan, K., 2013. Benzophenone-type UV filters in urine and blood from children, adults, and pregnant women in China: partitioning between blood and urine as well as maternal and fetal cord blood. Sci. Total. Environ. 461, 49–55.